Volume 1 | Number 1 | Jan 2013 | Pages 1–100

Journal of
Materials Chemistry B

Materials for biology and medicine
www.rsc.org/materialsB

ROYAL SOCIETY OF CHEMISTRY

This is an *Accepted Manuscript*, which has been through the Royal Society of Chemistry peer review process and has been accepted for publication.

Accepted Manuscripts are published online shortly after acceptance, before technical editing, formatting and proof reading. Using this free service, authors can make their results available to the community, in citable form, before we publish the edited article. We will replace this *Accepted Manuscript* with the edited and formatted *Advance Article* as soon as it is available.

You can find more information about *Accepted Manuscripts* in the **Information for Authors**.

Please note that technical editing may introduce minor changes to the text and/or graphics, which may alter content. The journal's standard **Terms & Conditions** and the **Ethical guidelines** still apply. In no event shall the Royal Society of Chemistry be held responsible for any errors or omissions in this *Accepted Manuscript* or any consequences arising from the use of any information it contains.

Cationic Liposomes as Efficient Nanocarriers for the Drug Delivery of an Anticancer Cholesterol-based Ruthenium Complex

Giuseppe Vitiello,[a,b] Alessandra Luchini,[b,c] Gerardino D'Errico,[b,c] Rita Santamaria,[d] Antonella Capuozzo,[d] Carlo Irace,[d] Daniela Montesarchio,[c,*] Luigi Paduano[b,c,*]

[a] Department of Chemical, Materials and Production Engineering, University of Naples "Federico II", Piazzale Tecchio 80, 80125 Naples – Italy.

[b] CSGI – Consorzio interuniversitario per lo sviluppo di Sistemi a Grande Interfase.

[c] Department of Chemical Sciences, University of Naples "Federico II", Via Cinthia 4, 80126 Naples, Italy.

[d] Department of Pharmacy, University of Naples "Federico II", Via D. Montesano 49, 80131 Naples, Italy.

*Corresponding Authors E-mail:

daniela.montesarchio@unina.it, luigi.paduano@unina.it

Phone: +39 081 674250. Fax: +39 081 674090.

Keywords: nanosystems; nucleolipid-based ruthenium (III) complex; cholesterol; microstructural characterization; cellular uptake; biological activity.

Abstract

Aiming at novel tools for anticancer therapy, a ruthenium complex, covalently linked to a cholesterol-containing nucleolipid and stabilized by co-aggregation with a biocompatible lipid, is here presented. The amphiphilic ruthenium complex, named ToThyCholRu, is intrinsically negatively charged and has been inserted into liposomes formed by the cationic 1,2-dioleyl-3-trimethylammoniumpropane chloride (DOTAP) so to hinder the degradation kinetics typically observed for known ruthenium-based antineoplastic agents. The here described nanovectors contain up to 30% in moles of the ruthenium complex and are stable for several weeks. This drug delivery system has been characterized using Dynamic Light Scattering (DLS), Small Angle Neutron Scattering (SANS), Neutron Reflectivity (NR) and Electron Paramagnetic Resonance (EPR) techniques. Fluorescence microscopy, following the incorporation of rhodamine-B within the ruthenium-loaded liposomes, shows fast cellular uptake in human carcinoma cells, with a strong fluorescence accumulation within the cells. The *in vitro* bioactivity profile reveals an important antiproliferative activity and, most remarkably, the highest ability in ruthenium vectorization measured so far. Cellular morphological changes and DNA fragmentation provide evidence of an apoptosis-inducing activity, in line with several *in vitro* studies supporting apoptotic events to explain the anticancer properties of ruthenium derivatives. Overall, these data highlight the crucial role played by the cellular uptake properties in determining the anticancer efficacy of ruthenium-based drugs, showing DOTAP as a very efficient nanocarrier for their stabilization in aqueous media and transport in cell. *In vitro* bioscreens have shown high antiproliferative activity of ToThyCholRu/DOTAP liposomes against specific human adenocarcinoma cell types. Furthermore, these formulations have proved to be over 20-fold more effective against MCF-7 and WiDr adenocarcinoma cells with respect to the nude ruthenium complex AziRu we have previously described.

Table of content

Cationic nanovectors loaded with ruthenium-based nucleolipids containing a cholesterol residue exert high growth-inhibitory activity against human cancer cells (MCF-7 (A), WiDr (B), and HeLa (C), before and after ToThyCholRu/DOTAP treatment).
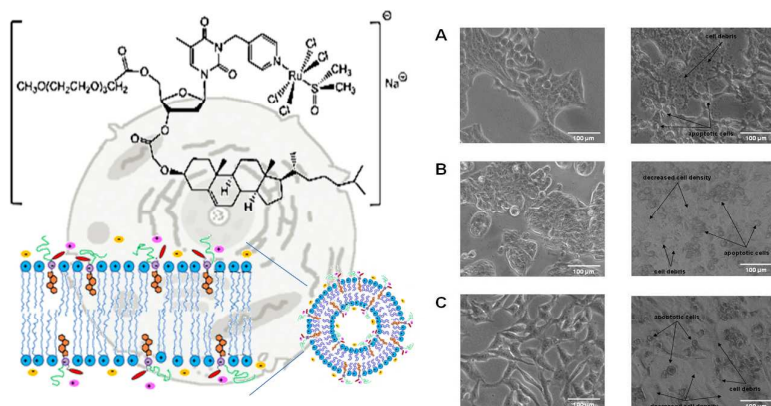
Introduction

Ruthenium coordination compounds have been proposed as potential anticancer agents because of their relevant antiproliferative activity.[1-3] In fact, they possess several favourable chemical properties that indicate them as strong antitumoral candidates in a rational drug discovery approach. In several cases, these compounds have been designed taking inspiration from bioactive Pt complexes, mainly cisplatin. Known since the mid 60's and approved by FDA as an anticancer agent in the late 70's, cisplatin[4] is still among the most widely used drugs for the treatment of several tumors,[5, 6] though its use is associated with severe side effects and its efficacy limited by primary and acquired resistance. Despite their general structural similarity with platinum complexes, ruthenium-based drugs have attracted great interest due to their lower toxicity, often associated with the ability to overcome the resistance encountered with platinum drugs.[7-9] The major advantages of ruthenium complexes are related to their peculiar features, as for example: i) the facility to exchange O- with N-donor ligands similarly to platinum-based drugs; ii) their octahedral geometry, which offers unique possibilities for the binding to nucleic acids; iii) the high versatility in terms of oxidation states, including II, III and perhaps IV in the biological fluids; iv) the possibility to be transformed into poorly reactive prodrugs, with the ruthenium ion in the +3 oxidation state that can be reduced, and thus activated, selectively in solid tumour masses as a result of their low oxygen content.[10]

Since the early 80's, Sava and coworkers have studied the transition metal complexes in a biomedical perspective, developing, among others, the ruthenium complex named NAMI-A, found to be a very active anticancer agent *in vitro*. This compound, along with KP1019 and RAPTA-C, has successfully completed Phase I,[11, 12] currently undergoing advanced Phase II clinical trials. In these compounds, similarly to cisplatin, the chloride ligands of the ruthenium complex can be replaced by hydroxide ions, leading to partial hydrolysis of the complex and poly-oxo species formation.[11, 12] Although the formation of poly-oxo species does not seem to significantly hamper the ruthenium bioactivity, at least when tested on some tumour cell lines,[13] a dramatic consequence of these degradation processes is that only a limited amount of the administered drug can be effectively internalized into cells.

In the context of the growing interest for ruthenium complexes in anticancer therapy, our group has recently proposed a novel approach for the *in vivo* delivery of ruthenium-containing drugs, based on their incorporation into suitable nucleolipid structures and successive co-aggregation with biocompatible lipids acting as nanovectors.[14-18]

Nucleolipids, being amphiphilic compounds, offer unique properties of spontaneous self-assembly providing nano-sized aggregates with exquisite tunability in terms of volume and shape.[14, 19, 20] The

insertion of ruthenium-containing structural motifs into amphiphilic building blocks may lead to efficient *in vivo* delivery and controlled release of the anticancer agents, thus producing a remarkable enhancement of their therapeutic efficacy. Following this concept, we have synthesized a set of novel ruthenium-based complexes able to spontaneously incorporate into the phospholipid membrane of a liposome.[14-18] As an evolution of our previous works, we here describe the molecular and microstructural characterization, along with detailed bioactivity studies, of the cholesterol-based ruthenium complex, named ToThyCholRu,[15] (Fig. 1), intrinsically negatively charged, when lodged in the biomimetic membranes formed by the cationic lipid 1,2-dioleoyl-3-trimethylammonium-propane (DOTAP), as shown in Fig. 1. Due to the high affinity of cholesterol with phospholipids, ToThyCholRu should easily penetrate into the cell membranes, thus facilitating the ruthenium complex internalization. Cholesterol is a fundamental component of cells membrane and, for this reason, the design and use of cholesterol-based lipids appears as a crucial step in the development of drug delivery research area. In the literature, different modifications of lipid architectures have been introduced at the headgroup level, headgroup-hydrophobic linker region and on the hydrophobic domains, in which cholesterol is directly involved.[21-23] These modifications can modulate their aggregation properties and the interactions with biological environment.[23, 24] Also, end-modification with a cholesterol motif has been successfully applied to biologically active oligonucleotides.[25] Notably, various liver[26] and spleen cell types easily take up antisense oligonucleotides conjugated with cholesterol.[27]

In our liposomes, the ruthenium complex anchored to the cholesteryl-functionalized nucleolipid is forcedly accommodated into the liposome bilayer, in a region where the contact with water or hydroxyl groups is limited, thus sensibly retarding the degradation kinetics. In a previous study, we have investigated ToThyCholRu when co-aggregated with the zwitterionic lipid POPC, and this system proved to be stable with the ruthenium complex contained up to 15% in moles.[15, 28] The here described amphiphilic liposomes, based on the cationic DOTAP, contain 30% in moles of ToThyCholRu, which at this composition is stable for several months.

The aggregation behaviour of liposomes, as well as their stability as a function of time, has been investigated through an experimental strategy proved extremely informative. It combines Dynamic Light Scattering (DLS) to estimate aggregate dimensions, Small Angle Neutron Scattering (SANS) to analyze the aggregate morphology and to determine their geometrical characteristics, Neutron Reflectivity (NR) to gain structural information on the bilayer and Electron Paramagnetic Resonance (EPR) to get information on the dynamics of lipid hydrophobic tails in the bilayer. Altogether, these investigations give detailed information on micro- and mesostructural

characteristics of these multifunctional liposomes, useful to cast light upon the mechanisms behind their cellular uptake and bioactivity.

Experimental data on the *in vitro* antiproliferative activity of these novel aggregates on human tumour and non-tumour cell lines are presented, showing a bioactivity enhancement of ca. one order of magnitude compared with previous results.[15] Finally, their uptake kinetics has been investigated by fluorescence microscopy, monitoring with time *ad hoc* prepared ruthenium-loaded liposomes incorporating a rhodamine B derivative.

Results and discussion

DOTAP liposomes in the absence and presence of the amphiphilic ToThyCholRu drug were suitably prepared by using the lipid film method and then suspended in the appropriate aqueous solution, as described in the experimental section.

Liposomes characterization by DLS, zeta-potential and SANS

In order to characterize the suspension of the aggregates composed by the lipid DOTAP and the ruthenium complex ToThyCholRu, both Dynamic Light Scattering (DLS) and Small Angle Neutron Scattering (SANS) experiments were performed. In particular, as shown in Fig. 2, a single broad population of aggregates resulted from the DLS analysis. This obtained distribution corresponds to the best fit to the measured correlation function with reproducible values from one experiment to another. The attempt to separate the single distribution in more distribution of aggregates of different size did not allow a reproducible result.[29] An accurate estimation of the mean hydrodynamic radius value was achieved performing measurements at different scattering angles. From the analysis of the collected data, reported in Fig. 3, the z-averaged diffusion coefficient, the polydispersity index and the mean hydrodynamic radius were calculated (see Table 1 and ESI). All the results obtained from the DLS characterization reflected the organization of the amphiphilic molecules into aggregates having the typical size of liposomes, as also observed for other formulations containing previously studied amphiphilic ruthenium complexes.[30]

The surface charge of liposomes was determined by zeta potential ζ measurements. This is a convenient parameter for characterizing the electrostatic properties of aqueous dispersions of colloidal particles such as micelles and vesicles that is strictly related to their mobility,[24] since ζ is a measure of the surface charge at slipping plane of the aggregates.[17] The ζ values confirm the formation of catanionic liposomes. Indeed, the positive surface charge carried by bare DOTAP vesicles (+41.7 mV± 1.5 mV) is partially neutralized by addition of negatively charged nucleolipid-

based Ru complexes (+37.2 ± 0.6 mV) . Similar effects were detected in another catanionic system made by nucleolipids and CTAB.[31]

The results obtained from the DLS characterization were completed by SANS measurements that confirmed the type of aggregates formed by DOTAP and ToThyCholRu, and allowed to determine other structural parameters. The model used to treat the experimental data accounts for a suspension of liposomes composed by a single lamella (see Fig. ESI2), uniformly contributing to the scattering intensity (Fig. 3). In particular, the neutron intensity profiles were treated according to the form factor of liposomes diluted solution with polydispersed thickness and uniform scattering length density (see equation 1 and Table 1):

$$I(q)=\frac{2\pi\left\{\frac{2\Delta\rho^2}{q^2}\left[1-cos(q\delta)\right]\right\}}{\delta q^2} \tag{1}$$

where δ is the bilayers thickness and $(\Delta\rho)$ is the contrast variation (see ESI for details). In the fitting procedure a variation of the bilayer thickness value (σ) obeying to a gaussian distribution was also considered. In Table 1 the polydispersity index obtained, PD = σ/δ is reported (see ESI for details).

The fitting of the applied model showed a good agreement with the experimental data and the cryo-TEM image (see Fig. ESI3), and thus no contribution of a structure factor was considered confirming the presence of diluted unilamellar liposomes within the sample.

Bilayer microstructural characterization by NR and EPR

Lipid bilayers of pure DOTAP and ToThyCholRu/DOTAP were characterized by Neutron Reflectivity (NR) using different isotopic contrast solvents. This technique allows to determine the structure and composition of layers at interfaces, furnishing detailed information on the bilayer microstructure and lipids organization.[32, 33]

The experimental curves are shown in Fig. 4 and the parameters used to fit the curves simultaneously from all the contrasts are given in Table 2. For all lipid systems, a five box model was found to best fit the data. The first two boxes correspond to the silicon block and to the thin solvent layer interposed between the silicon surface and the adsorbed bilayer. The other three boxes describe the bilayer, which is subdivided into the inner headgroups, the hydrophobic chains, and the outer headgroups layers. For all considered bilayers, a model without the water layer between the

substrate and the bilayer gave a worse fit to the data. The theoretical scattering length density (ρ) values of the used lipids were calculated through equation 2 and are reported in Table ESI1:

$$\rho(z) = \sum_j n_j(z) b_j \qquad (2)$$

where $n_j(z)$ is the number of nuclei per unit volume and b_j is the scattering length of nucleus j. [34]

Thus the parameters obtained from the best fit procedure are the thickness and the roughness of each box, plus the solvent content expressed as volume percent (see Table 2). We note that the roughness is related to the compactness of each bilayer region: large values of the fitting number correspond to more dense layers. Generally, the roughness values cannot be higher than the thickness ones. The presence of ToThyCholRu in DOTAP bilayers influences their microstructure. First, the variation in the ρ values corresponding to all bilayer regions clearly indicates the insertion of ToThyCholRu molecules in DOTAP bilayers. In detail, this insertion causes an increase of the hydrophilic region thickness of 4 ± 1 Å, while the hydrophobic region is similar to that obtained for pure DOTAP. Moreover, in the case of bilayers containing ToThyCholRu, the hydrophilic region is characterized by a slight increase of the solvent content, depending on the different packing density induced by ruthenium complex molecules, which causes a higher compactness in the DOTAP bilayer. No changes have been observed in the roughness values. These results are in agreement with those obtained for the ToThyCholRu/POPC bilayers. [15]

Spin-label EPR spectroscopy has been proved to give substantial information on the acyl chains structuring and dynamics in the lipid bilayers. [35-37] In this study, different spin-labels were alternately used. They present a nitroxide group, positioned at the levels of the 5, 7, 10, and 14 carbon atom of a phosphocholine backbone of a *sn*-2 chain, called *n*-PCSL (see Fig. ESI1). The former bears the radical nitroxide group close to the hydrophilic moiety of the molecule, while in the latter the reporter group is located at the end of the hydrophobic tail. Consequently, 5- and 7-PCSL provide information on the aggregate microdomain just below the external surface, while the 10- and 14-PCSL give information on the inner core. The goal has been to investigate how the DOTAP membrane fluidity is influenced by the presence of ToThyCholRu at 70:30 molar ratio.

EPR spectra of spin- labels in bilayers of ToThyCholRu/DOTAP liposomes at 30:70 molar ratio are shown in Fig. 5. In the same figure, the EPR spectra of the spin-labels in pure DOTAP vesicles are also presented. The spectra show an anisotropic lineshape for 5-PCSL and an almost isotropic lineshape in the case of 14-PCSL. This is a characteristic hallmark of lipid bilayers in the liquid-crystalline fluid phase. [38] A quantitative analysis of the spectra has been performed by determining

the order parameter, S, and the coupling hyperfine constant, a'_N, whose values are reported in Table 4. S is a measure of the local orientational ordering of the labelled molecule with respect to the normal to the bilayer surface, while a'_N is an index of the micropolarity experienced by the nitroxide. Both S and a'_N decrease progressively with increasing n, as the spin-label position is stepped down the chain toward the center of the membrane.[39]

Spectra of the spin-labels at 70:30 molar ratio in Fig. 5, together with the order parameter (S) corresponding values in Table 3, show that the presence of ToThyCholRu in the DOTAP liposomes bilayers causes an increase of the order parameter, S, for all n-PCSL spin-labels indicating a stiffening effect on the whole lipid bilayer carbon atoms closer to the hydrophilic region of the complex. In particular, a strong increase is detected in the S value of 14-PCSL, which indicates that the presence of the cholesterol scaffold induces an increase in lipid packing density of the inner chains region. It is interesting to note that pure cholesterol reduces dynamics and increases order of the whole lipid acyl chains in DOTAP bilayers, as indicated by the S values reported in Table 4 (DOTAP/Chol column). In particular, the comparison of the data relative to ToThyCholRu/DOTAP with those of DOTAP/Chol bilayers suggests that the cholesterol residue positioning in the bilayer is the same for the two systems. Furthermore, pure cholesterol causes a higher effect on the DOTAP bilayers than ToThyCholRu and this could be probably due to the headgroup of ToThyCholRu, which to a minor extent influences the lipid packing density of the more external region ($5 \leq n \leq 10$) compared to cholesterol, which particularly affects the acyl chain mobility ($n \geq 14$).

Concerning a'_N, it appears that its value is only marginally affected by the ruthenium complex. In particular, ToThyCholRu causes a slight increase in the local polarity, indicating a higher content of water in the external headgroup region, which is a consequence of the increased ordering and compactness induced by the presence of the ruthenium complex molecules. These results are in agreement with NR data (Fig. 6). Finally, EPR spectra, performed on the same samples after three months, showed no variation of the signals, confirming the stability with time of the bilayers formed by DOTAP hosting ToThyCholRu.

Cellular uptake studies

The internalization and accumulation of the metal-based drugs into cancer cells is crucial for the therapeutic effect against tumors.[40] A large number of metallomic and biological investigations have been conducted primarily on cisplatin and its derivatives, but more recently also on metals compounds alternative to platinum such as ruthenium, showing DNA as an important target of these drugs.[41, 42] While it is widely accepted that binding to DNA is the main mechanism for platinum-

induced cytotoxicity,[43] nuclear and cytosolic proteins have as well moved into attention as potential targets for ruthenium-based drugs.[44, 45]

In view of more detailed investigations on the interactions of these liposomes with protein targets, we have first analyzed their interaction with cell membranes and cell internalization processes. To this aim, a standardized protocol based on a rhodamine B fluorescent probe loaded into DOTAP/ToThyCholRu liposomes has been used to evaluate their uptake in human carcinoma cells.[17] In order to determine the impact of incubation times on the ToThyCholRu accumulation within the cells, uptake experiments were carried out at 100 μM concentration and at incubation times of 30 min, 1, 3 and 6 h on human MCF-7 breast and WiDr colorectal adenocarcinoma cells, and the corresponding results are depicted in Fig. 7 and 8, respectively. In the microphotographs, the blue areas correspond to the cells nuclei specifically stained by DAPI, whereas the rhodamine (RHOD) associated fluorescence within cells is shown in green. As described in our previous report, the fluorescence emission herein reported in green is produced by a rhodamine B lipid derivative added as a fluorescent probe at 2% molto the liposomes. Control experiments have been also performed by exposing the cells to the rhodamine B adduct alone under the same *in vitro* experimental conditions used to evaluate the cellular uptake of ruthenium-containing liposomes. Merged images arise by overlapping fluorophores emission emerging from the same cell monolayers. The cationic ToThyCholRu/DOTAP liposome rapidly interacts with biological membranes allowing a massive cellular uptake, even after short incubation times such as 30 min and 1 h. The rhodamine-dependent fluorescence emission is localized widespread in the cells and merged images show a strong fluorescence accumulation both in MCF-7 and WiDr. In a process of cell internalization that probably occurs by nonspecific patterns *via* membrane fusion and/or endocytosis, the presence of a cholesterol motif within the amphiphilic structure decorating the ruthenium complex in ToThyCholRu could further improve the liposome fusion with the plasma membrane, thus promoting strong nanocarriers accumulation within the cells. Due to the high affinity of cholesterol for phospholipids, several *in vitro* evidences concerning liposomes interaction with membrane show a specific cholesterol/lipid ratio - similar to the one reported for the plasma membrane of animal cells - to obtain the optimal fusion.[46, 47] In addition to the amphiphilic properties of ToThyCholRu complex, the liposome membranes formed by the cationic lipid DOTAP allow the onset of charge attraction that could play an important role in promoting close contact with the negatively charged target membrane.[48]

Overall, these data are consistent with our previous cellular uptake findings carried out on the first generation of ruthenium (III) complexes lodged both in POPC and DOTAP liposomes.[16, 17] Moreover, they support the results of a more recent investigation on a novel ruthenium(III)

complex, named HoUrRu, which exhibits higher antiproliferative activity when the ruthenium(III) complex is mixed with the cationic lipid DOTAP than when aggregated with the zwitterionic POPC.[18]

In vitro bioscreening for anticancer activity

The cytotoxic profile of the ruthenium-containing nanocarrier was investigated *via* bioscreening on a selected panel of human cancer cells following 48 h of incubation. As well as in *in vivo* testing, drug-dependent biological effects on cultured cells usually occur after a time range starting from treatments *in vitro*. Indeed, despite effective and fast processes of cellular uptake, the elapsing time (latency) between the drug administration and the onset of pharmacological effect and its duration, both *in vitro* and *in vivo*, may depend on many factors. Moreover, biological responses virtually mediated by the activation of cell death/cell stopping pathways and complex changes in cell cycle kinetics represent an even more complicated condition. According to our previous reports, an *in vitro* time range of 36-48 h between the cellular uptake and the occurrence of biological effects may normally elapse. This scenario is consistent with both the metal-induced antiproliferative effects and the cell population doubling time, that for instance is approximately 38 h for MCF-7 cells. [49]

In line with our project, the experimental procedure involves the estimation of the ToThyCholRu/DOTAP anticancer activity by a "cell survival index", deriving from evaluation of the cellular metabolic activity (MTT colorimetric assay) and monitoring of live/dead cells ratio (trypan blue exclusion assay), as described in the experimental section. The results are reported both in concentration-effect curves (Fig. 9) and in terms of IC_{50} values (Table 4). Data concerning the low molecular weight ruthenium complex AziRu are included for comparison, as well as data for cisplatin (*c*DDP) - a positive control for cytotoxic effects - and for the previously investigated ToThyCholRu/POPC system.[15] Similarly, ruthenium-free ToThyChol/POPC and ToThyChol/DOTAP liposomes have also been added in these bioscreens as negative controls to better understand and discuss the results. AziRu – depicted in Fig. 1, along with the nucleolipid ToThyChol - is the NAMI-A-inspired molecular core of our mini-library of amphiphilic ruthenium-containing molecules, which has been proved by us[15] and others[50] to be endowed with higher antitumor activity than NAMI-A itself, which is known to act primarily as an antimetastatic agent.[51] The results show that ToThyCholRu/DOTAP exhibits an interesting bioactivity pattern characterized by selective cytotoxicity against highly proliferative malignant cells. In fact, different histological human adenocarcinoma cells, such as MCF-7, WiDr and HeLa, undergo remarkable antiproliferative effects following incubations with the ruthenium-based complex, while no

significant cytotoxicity has been detected on non-cancer human HaCaT keratinocytes and rat L6 muscle cells. Within this context, the evaluation of *c*DDP and ruthenium-based complexes effects on non-cancer control cultures (see the related IC_{50} values in Table 4) deserves a further insight. Since most anticancer drugs lack tumor specificity and cause damage to normal tissues, with heavy side effects, ruthenium complexes may provide a less toxic and more effective alternative to common therapies. Indeed, new ruthenium-based compounds with less severe side effects could replace longstanding metal-based anticancer drugs as cisplatin and its derivatives. Consistently with our previous reports, the cell survival decreases already at very low concentration of the active ruthenium in breast adenocarcinoma cells (MCF-7 line, Fig. 9, panel A). Taking into account that ruthenium is incorporated in 30% in moles in the DOTAP liposomes under investigation, concentration-effects curves related to the actual ruthenium content throughout bioscreens, reported in the right column of Fig. 9, strongly emphasize the high anticancer activity of the ToThyCholRu/DOTAP system. Since pure DOTAP and POPC liposomes,[16,17] as well as both the ruthenium-free liposomes in DOTAP and POPC (ToThyChol/DOTAP and ToThyChol/POPC, respectively) do not interfere with the *in vitro* bioassays, inhibition of cell growth and proliferation can be exclusively attributed to the presence of ruthenium.

IC_{50} values are close to the 10 µM range for MCF-7 cells and somewhat higher for WiDr and HeLa cells. In general, these results indicate that the following order of *in vitro* antiproliferative activity can be considered: ToThyCholRu/DOTAP ≥ cisplatin > ToThyCholRu/POPC > AziRu.

ToThyCholRu/DOTAP is more potent than cisplatin against two of the three cancer cell lines here tested (approximately 1.7 and 1.4-fold more potent than cisplatin in killing MCF-7 cells and WiDr, respectively), while cisplatin remains more effective in stopping HeLa cells proliferation. As mentioned earlier, it is noteworthy that ruthenium cytotoxicity against the normal HaCaT and L6 cells is very low, in addition being always lower than that of cisplatin.

The observed antiproliferative effects of the ToThyCholRu/DOTAP system on tumor cells are largely consistent with its intracellular uptake properties and show that the amphiphilic nature of the synthesized ruthenium (III) complex, and the consequent self-aggregation, do not perturb the metal-induced biological effects. Although broadly in line with the activities of the amphiphilic ruthenium-containing molecules we have previously described, the calculated IC_{50} for ToThyChol/DOTAP are significantly lower than those related to the same nucleolipidic ruthenium (III) complex lodged in neutral POPC liposomes. This means that, under identical *in vitro* experimental conditions, the use of cationic DOTAP liposomes as nanocarrier for ToThyCholRu greatly enhances its anticancer activity.

Indeed, in the transition from ToThyCholRu/POPC to ToThyCholRu/DOTAP the potentiating factor (PF) values for ruthenium vectorization with respect to the precursor molecule AziRu in MCF-7 and WiDr cells increases from 4.3 and 3.1 to 23.5 and 22.4, respectively, reaching the highest values we have measured hitherto this project. Thus in MCF-7 cells - the most responsive ones to ruthenium action in our *in vitro* models - the same antiproliferative effect of the precursor complex AziRu is achieved in the case of ToThyCholRu in POPC, with a metal concentration 6-fold lower, and in the case of ToThyCholRu in DOTAP, with a metal concentration 10-fold lower. These data further emphasize the main role played by the drug delivery systems in influencing the cellular uptake properties and, thus, the antiproliferative efficacy of metal-based anticancer drugs.

Cellular morphological changes and DNA fragmentation

The results herein presented demonstrate that ruthenium-based nucleolipids containing a cholesterol residue and loaded in cationic DOTAP liposomes exert high growth-inhibitory activity against cultured human cancer cells. To further support the relationship between cell viability and ruthenium-induced cytotoxicity, subconfluent cultures of MCF-7, WiDr and HeLa cells have been examined by phase-contrast light microscopy for the dynamic cell population monitoring of the morphological changes that occur during cell death. Following the *in vitro* exposure to ToThyCholRu/DOTAP, morphological modifications of the cell monolayers clearly appear (Fig. 10). In particular, microscopy provides evidence that the reduction in cell viability by ruthenium-based nanocarriers application is associated with well detectable cytotoxic effects and distinctive morphologic hallmarks of apoptosis. The onset of apoptosis is characterized by membrane blebs and cell shrinkage, and culminates with formation of balloon-like structures indicating the loss of plasma membrane integrity.[52] Besides losing their normal morphological features, the rounding up of the cells visibly increased after 48 h of incubation, with enhancement of the surface blebbing and cell shrinkage.[53]

In addition, late events of apoptosis include nuclear pycnosis and DNA cleavage, resulting in the DNA fragmentation visualized as a 'ladder' by agarose gel electrophoresis. Thus DNA fragmentation extent detected in cultured cells typically exhibits a direct correlation with the amount of apoptotic cells present in cultures, scored morphologically by microscopic analysis. In Fig. 11 untreated cancer cells showed no detectable DNA fragmentation, whereas DNA extracted from cells after 48 h of incubation with IC_{50} doses of both ToThyCholRu/DOTAP and *c*DDP was extensively fragmented. It is very interesting to note the atypical fragmentation pattern of damaged DNA shown by MCF-7 cells after these *in vitro* treatments. Indeed, MCF-7 is one of the human breast cancers known to be resistant to some chemotherapeutics due to deletion in the CASP-3 gene

that leads to an inherited deficiency of caspase-3.[54] Caspase-3, commonly activated by numerous death signals, cleaves a variety of important cellular proteins and is ultimately responsible for apoptotic DNA fragmentation. It has been also reported that MCF-7 undergoes cell death by apoptotic stimuli in the absence of DNA fragmentation, as well as recent observations further suggest large and small DNA fragments coupled to even single-strand cleavage events occurring during apoptotic cell death. These observations have raised many questions on the appearance of the fragmentation pattern by gel electrophoresis detection that remains controversial. However, morphological changes and MCF-7 cell death were independent of caspase-3 and may correlate with the activation of different apoptotic pathways and other effector caspases, such as caspase-6 or -7.[55] In contrast, treatment of WiDr and HeLa cells with ToThyCholRu/DOTAP resulted in the appearance of the internucleosomal DNA laddering typical of cells undergoing apoptosis. This effect is similar to that induced *in vitro* by IC_{50} doses of *c*DDP, likely *via* caspase-3 activation.[56] Although the implication of various molecular pathways involved in cell death processes cannot be excluded, these outcomes provide evidence of an apoptosis-inducing activity, in line with several *in vitro* studies supporting apoptotic events to explain the anticancer properties of different types of ruthenium derivatives.[57, 58]

Experimental

Materials

DOTAP phospholipid, spin-labeled phosphatidylcholines (1-palmitoyl-2-[n-(4,4-dimethyloxazolidine-N-oxyl)]stearoyl-*sn*-glycero-3-phosphocholine, *n*–PCSL, *n*= 5,7,10,14) and 1,2-dioleoyl-sn-glycero-3-phosphoethanolamine-N-(lissamine rhodamine B sulfonyl) were purchased from Avanti Polar Lipids. D_2O (isotopic enrichment > 99.8%, molar mass 20.03 g mol^{-1}) was purchased from Aldrich.

Synthesis of the ruthenium complex ToThyCholRu

The investigated ruthenium complex, named ToThyCholRu, was prepared by reacting in stoichiometric amounts the starting nucleolipid, named ToThyChol,[59] with the Ru complex [*trans*-RuCl$_4$(DMSO)$_2$]$^-$Na$^+$ following a previously described procedure.[15] The desired salt was obtained in a pure form, as confirmed by TLC and ESI-MS analysis, and almost quantitative yields.

Lipid-based aggregates preparation

The samples containing ToThyCholRu were dissolved in a pseudo-physiological solution whose composition is specified hereafter. For the samples containing DOTAP and ToThyCholRu, the

following standard procedure to form vesicles was applied: weighed amounts of ToThyCholRu and DOTAP were dissolved in chloroform. Then, the solutions were transferred in round-bottom glass tubes and a thin film of the solutes was obtained through evaporation of the solvent with dry nitrogen and keeping the samples under vacuum for at least 24 h. The film was then hydrated with H_2O or a pseudo-physiological solution. This was prepared in double distilled and degassed water dissolving appropriate amounts of NaCl and KH_2PO_4 so that their final concentration was 0.140 mol dm^{-3} and 0.010 mol dm^{-3}, respectively.

Samples for SANS measurements were prepared in heavy water (D_2O, isotopic enrichment > 99.8%, molar mass 20.03 g mol^{-1}) in order to minimize the incoherent contribution to the scattering cross sections arising from the system.

For the samples to be analyzed through SANS and DLS, after sonication the suspension were repeatedly extruded through polycarbonate membranes of 100 nm pore sized, for at least 15 times.

Samples prepared for EPR experiments also included 1% (w/w) of spin-labeled phosphatidylcholine (1-palmitoyl-2-[n-(4,4-dimethyloxazolidine-N-oxyl)]stearoyl-*sn*-glycero-3-phosphocholine, *n*–PCSL, *n*= 5,7,10,14), purchased from Avanti Polar Lipids and stored at –20 °C in ethanol solutions. Inclusion of *n*-PCSL did not affect the liposome mesostructure as confirmed by DLS analysis of the aggregates dimension.

For NR experiments, Supported Lipid Bilayers (SLBs) were prepared by vesicles fusion: Small Unilamellar Vesicles (SUVs), of 25-35 nm in diameter, were formed by vortexing and sonicating for 3×10 min the MLVs suspension. The SUVs suspension (0.5 mg ml^{-1}) was injected into the NR cell, allowed to diffuse and adsorb on the silicon surfaces over a period of 30 min. The solid supports for neutron reflection were 8×5×1 cm^3 silicon single crystals cut to provide a surface along the (111) plane, and pre-treated. After lipid adsorption the sample cell was rinsed once with deuterated water to remove excess lipid.

Samples for fluorescence microscopy were prepared as reported above by adding 2% mol of 1,2-dioleoyl-sn-glycero-3-phosphoethanolamine-N-(lissamine rhodamine B sulfonyl) ammonium salt, here abbreviated as Rhod, purchased from Avanti Polar Lipids and used as received.

Conclusions

In the context of an intense search for metallodrugs alternative to platinum-based clinically validated anticancer agents, the growing interest for ruthenium derivatives has recently prompted us to synthesize a mini-library of ruthenium complexes coordinated by differently decorated nucleolipids. These derivatives have typically showed a marked propensity for aggregation in

aqueous solutions and high *in vitro* antiproliferative activity against human cancer cells. Within this project, we have herein reported on the molecular and microstructural characterization, along with a detailed bioactivity profiling, of the cholesterol-containing ruthenium complex, named ToThyCholRu, which is intrinsically negatively charged, accommodated into the liposome bilayers formed by the cationic lipid DOTAP. In order to develop stable and long-life carriers containing significant amounts of the active metal, the co-aggregation with biocompatible lipids represents an innovative strategy for the *in vivo* delivery of ruthenium-containing drugs. Interestingly, in contrast with known ruthenium complexes currently in clinical trials as anticancer agents, the ToThyCholRu/DOTAP liposome is stable for several months, further ensuring the complete integrity of the active ruthenium complex in physiological environment. *In vitro* bioscreenings converge in showing high antiproliferative activity, with ToThyCholRu/DOTAP exhibiting a cells killing ability higher than cisplatin against specific human adenocarcinoma cell types. Worth mentioning, in the transition from the previously investigated ToThyCholRu/POPC to the here described ToThyCholRu/DOTAP system, considerable progress has been achieved. In fact, the potentiating factors for ruthenium vectorization reach the highest levels we have measured hitherto this project, with ToThyCholRu/DOTAP proving to be over 20-fold more effective against MCF-7 and WiDr adenocarcinoma cells than the reference drug AziRu, a low molecular weight ruthenium-complex we have developed as NAMI-A analog. Consistently with our previous investigations, these outcomes designate the biocompatible DOTAP as a very valuable tool in nanobiotechnological applications, suitable as efficient nanocarrier for nucleolipid ruthenium complexes stabilization in aqueous media and transport in cell. Actually, by means of an *ad hoc* designed liposome including a fluorescent rhodamine-B probe, an efficient and fast liposomes accumulation has been detected in cells, further highlighting the physico-chemical properties and cellular uptake characteristics exhibited by these ruthenium-based drugs as critical features in determining their antiproliferative efficacy. In this context, an important role is played by the positive net superficial charge of the aggregates, as well as by the steroid moiety of the nucleolipid complex inserted in the acyl chain region. In fact, in addition to favoring the inclusion of the amphiphilic molecule inside the DOTAP liposome bilayer - thus protecting the ruthenium complex from degradation - cholesterol is believed to play a major role in cell uptake processes for its ability to regulate the physico-chemical properties of lipid bilayers, to stabilize liposomes and to modulate membrane trafficking by improving the liposome fusion with the plasma membrane.

In conclusion, our study shows that the co-aggregation of nucleolipid ruthenium complexes with the cationic lipid DOTAP has a great potential for developing new ruthenium-based anticancer drug candidates. Particularly, the cholesterol-containing ToThyCholRu/DOTAP aggregate here proposed

exhibits a remarkable cytotoxicity and selectivity toward specific cancer cell types. These findings suggest relevant specificity in the molecular interactions of ruthenium, in its active form, with the biological targets. Further structure–activity relationship studies are currently in progress in order to clarify these aspects and to investigate the *in vivo* antitumoral activity of nucleolipidic ruthenium (III) complexes.

TABLES

Table 1: Results obtained from the DLS and SANS measurements. In particular the first two columns refer to the parameter obtained from the treatment of the data reported in Fig. 2, while the third column shows data calculated from equation 3. The latter two columns refer to the parameters obtained by treating the SANS experimental data with the lamellar phase model.

$\langle D \rangle_z$ $(cm^2 \cdot s^{-1})$	$\langle R_h \rangle$ (nm)	δ (nm)	δ^*
$(3.07 \pm 0.06)\ 10^{-8}$	80 ± 2	3.2 ± 0.3	0.42 ± 0.01

Table 2 - Parameters derived from model fitting the reflectivity profiles for pure DOTAP lipid bilayers[17] and coaggregates ToThyCholRu/DOTAP complex.

DOTAP	interfacial layer	thickness (Å)	% solvent content	roughness (Å)
	water	6 ± 1	100	5 ± 1
	inner headgroups	10 ± 1	21 ± 10	4 ± 1
	chains region	25 ± 2	8 ± 10	7 ± 1
	outer headgroup	9 ± 1	47 ± 10	4 ± 1
ToThyCholRu/DOTAP	**interfacial layer**	**thickness (Å)**	**% solvent content**	**roughness (Å)**
	water	5 ± 1	100	5 ± 1
	inner headgroups	7 ± 1	46 ± 10	4 ± 1
	chains region	27 ± 2	5 ± 10	2 ± 1
	outer headgroup	13 ± 1	51 ± 10	4 ± 1

Table 3 - S and a'_{N} values of n-PCSL in liposomes of DOTAP, ToThyCholRu/DOTAP 30:70 mol/mol and DOTAP/Chol 70:30 mol/mol at 25 °C.

n-PCSL	S		
	DOTAP	**ToThyCholRu/DOTAP**	**DOTAP/Chol**
5-PCSL	0.59 ± 0.01	0.66 ± 0.01	0.73 ± 0.01
7-PCSL	0.55 ± 0.01	0.61 ± 0.01	0.67 ± 0.01
10-PCSL	0.49 ± 0.02	0.53 ± 0.02	0.58 ± 0.01
14-PCSL	0.15 ± 0.02	0.38 ± 0.02	0.37 ± 0.02

n-PCSL	a'_{N} /G		
	DOTAP	**ToThyCholRu/DOTAP**	**DOTAP/Chol**
5-PCSL	15.3 ± 0.1	15.6 ± 0.1	15.7 ± 0.1
7-PCSL	15.2 ± 0.1	15.5 ± 0.1	15.4 ± 0.1
10-PCSL	15.1 ± 0.2	15.1 ± 0.2	15.0 ± 0.1
14-PCSL	14.0 ± 0.2	14.1 ± 0.2	14.1 ± 0.2

Table 4 - Comparison of the IC_{50} values (μM) relative to cisplatin (*c*DDP), AziRu, and to the effective metal concentration carried by ToThyCholRu/POPC and ToThyCholRu/DOTAP liposomes in the indicated cell lines following 48 h of incubation[a]. In bold are indicated the Potentiating Factors (PF) of the ruthenium complexes in POPC or in DOTAP liposomes with respect to AziRu [b].

Cell lines	cDDP	AziRu	ToThyCholRu POPC	ToThyCholRu DOTAP
MCF-7	22 ± 4	305 ± 16	70 ± 12 **4.3**	13 ± 2 **23.5**
WiDr	32 ± 5	515 ± 15	165 ± 10 **3.1**	23 ± 8 **22.4**
HeLa	12 ± 4	382 ± 19	105 **3.6**	34 ± 4 **11.2**
HaCaT	272 ± 7	> 500	> 500	377 ± 2.5
L6	52 ± 6	> 500	> 500	187 ± 1

[a] IC_{50} values are reported as mean ± SEM (*n* = 30) of five independent experiments.
[b] P.F. are calculated as the ratio of IC_{50} values of ToThyCholRu/POPC and ToThyCholRu/DOTAP liposomes with respect to the IC_{50} of AziRu.

Figures
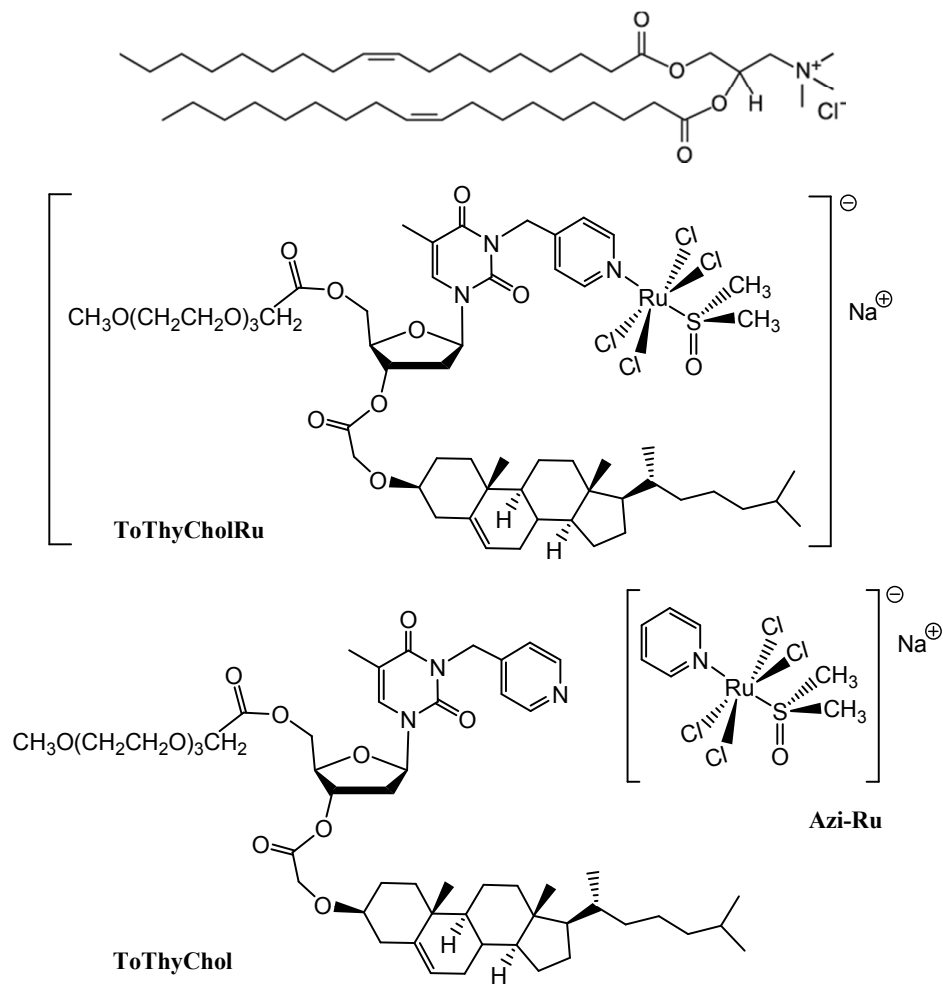
Fig. 1. Molecular structures of DOTAP phospholipid and of the ruthenium complexes ToThyCholRu and AziRu, as well as of the nucleolipid ToThyChol.
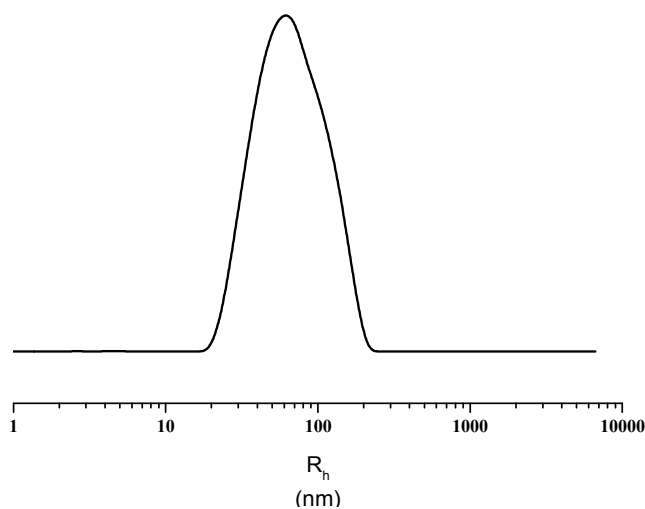
Fig. 2. Intensity weighed hydrodynamic radius distribution of ToThyCholRu/DOTAP liposomes. The distribution was obtained from one of the DLS measurements performed with the instrumental configuration corresponding to a scattering angle of 90°. This distribution showed the existence of a single population of aggregates within the suspension.
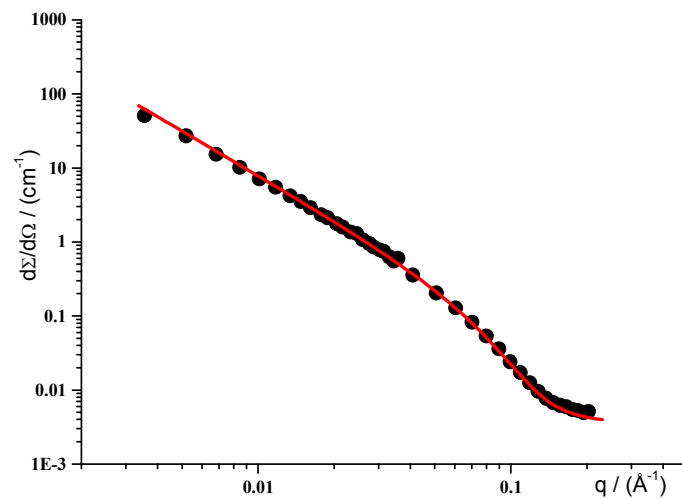
Fig. 3. Neutron scattered intensity data and the relative fitting curve, using the model of a diluted unilamellar vesicles suspension.
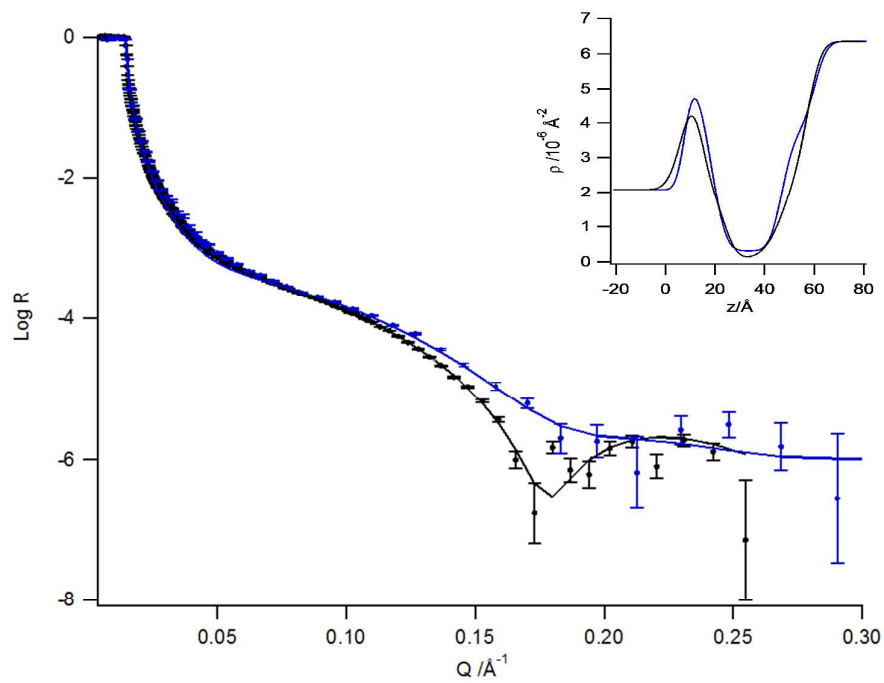
Fig. 4. Neutron reflectivity and scattering length density, ρ, profiles for lipid bilayers of DOTAP (black line) and ToThyCholRu/DOTAP30:70 mol/mol(blue line) in D_2O contrast solvent.
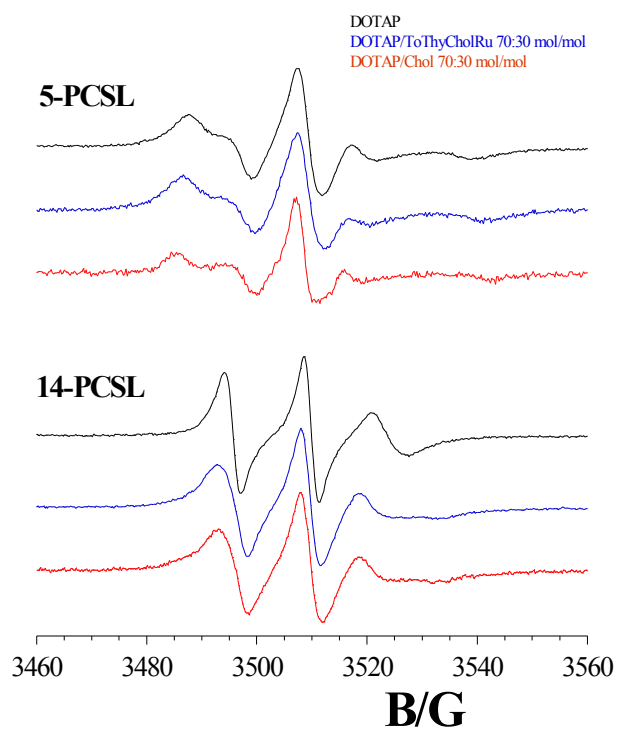
Fig. 5. EPR spectra of 5-PCSL and 14-PCSL spin-labels in bilayers of pure DOTAP (black lines), DOTAP:Chol 70:30 mol/mol (red lines) and in ToThyCholRu/DOTAP 30:70 mol/mol (blue lines).
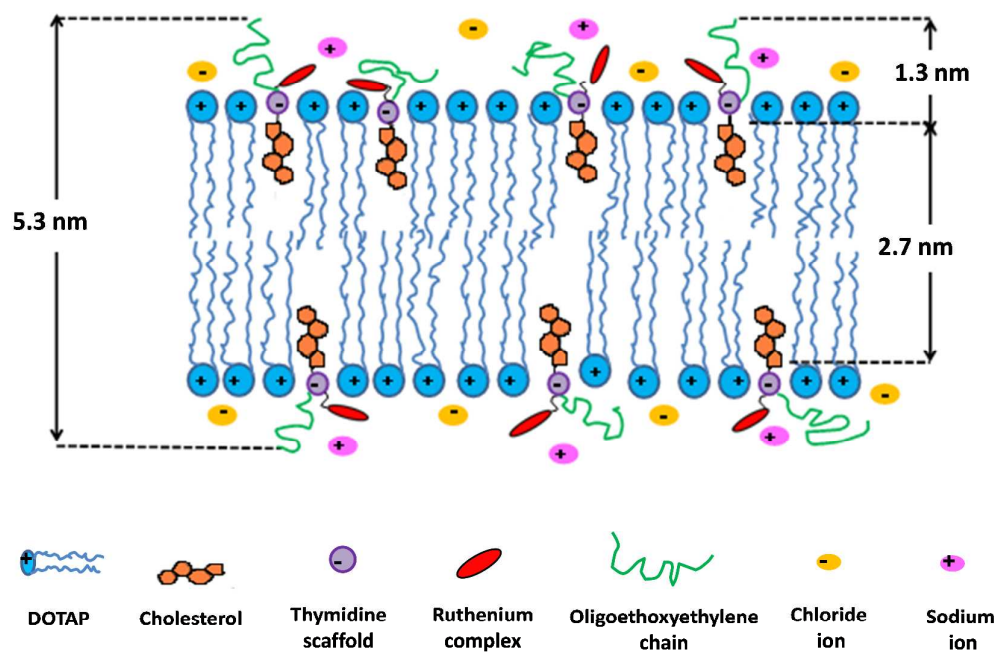
Fig. 6. Graphical representation of the bilayer structure constituting the lipid nanovectors.
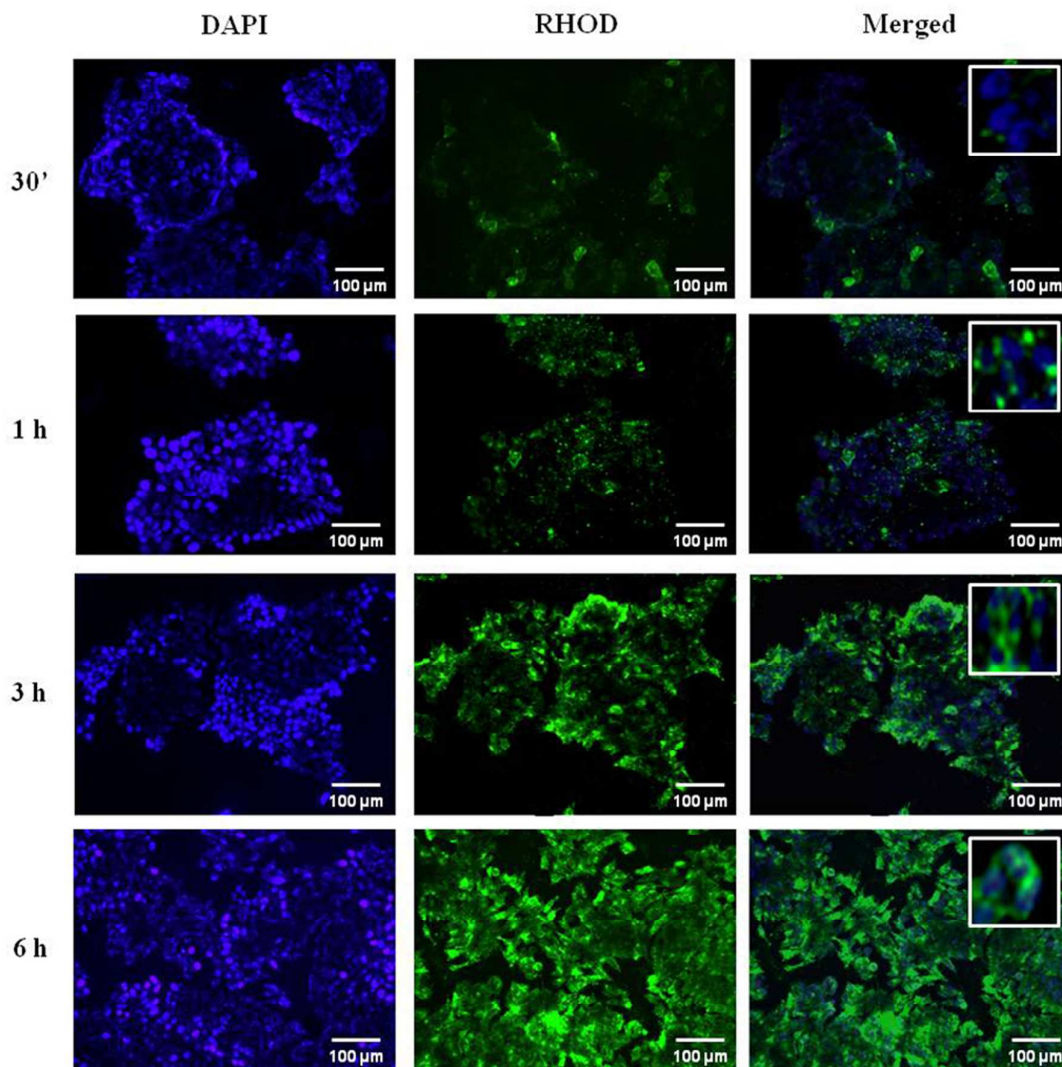
Fig. 7. Uptake of ToThyCholRu/DOTAP liposomes by human MCF-7 breast adenocarcinoma cells incubated for 30 min, 1, 3 and 6 h with a 100 μM solution of the liposomes containing a rhodamine B lipid derivative as fluorescent probe. The blue-fluorescent DAPI specifically stains the nuclei. The rhodamine-dependent fluorescence (RHOD, shown in green) exclusively stains the ToThyCholRu/DOTAP liposomes. In merged microphotographs (Merged), the two fluorescent patterns are overlapped. The shown images are representative of three independent experiments. 100× total magnification (10 × objective and a 10 × eyepiece). Inset: higher magnifications of merged images showing rhodamine-dependent cytoplasmic fluorescence emission by cell monolayers.
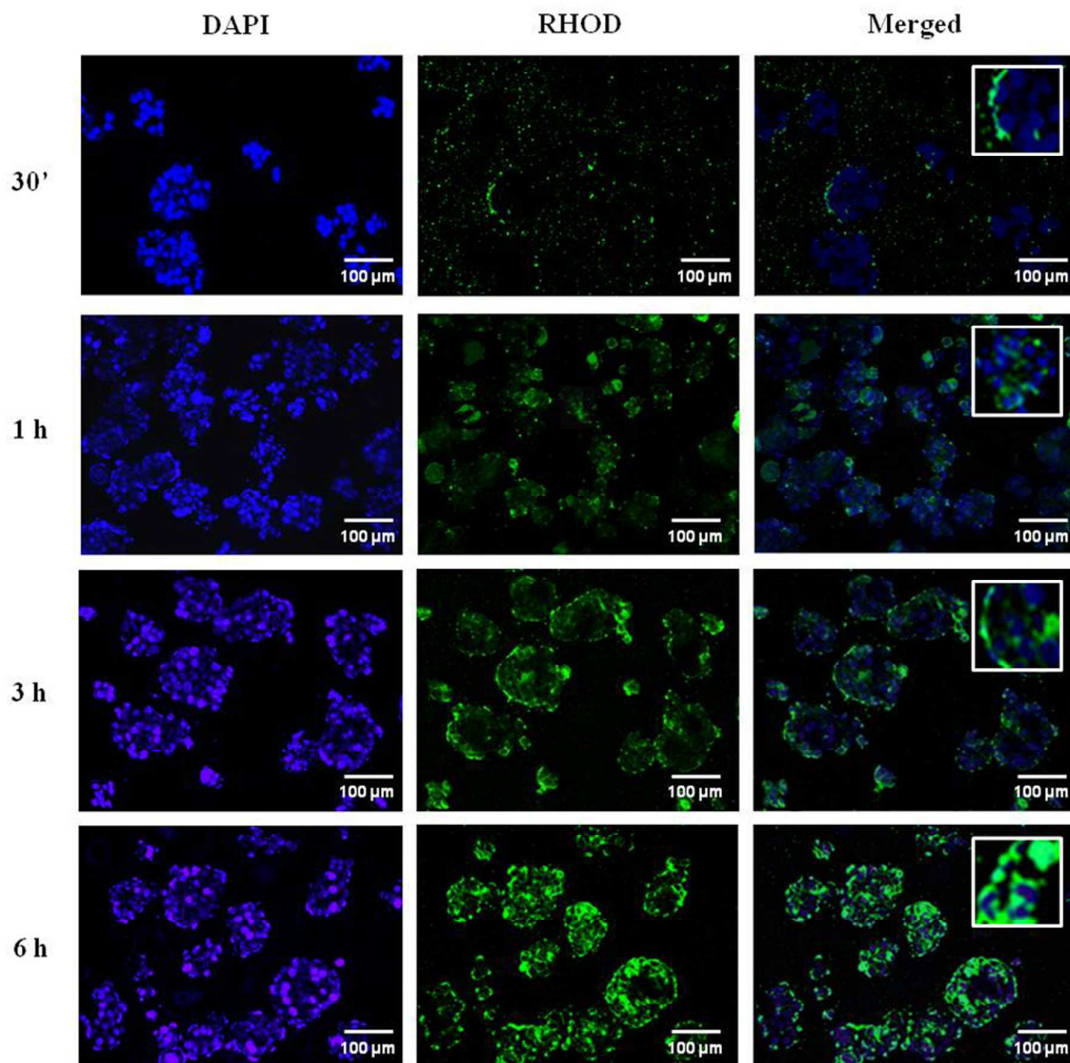
Fig. 8. Uptake of ToThyCholRu/DOTAP liposomes by human WiDr colorectal adenocarcinoma cells incubated for 30 min, 1, 3 and 6 h with a 100 μM solution of the liposomes containing a fluorescent rhodamine B lipid derivative, as described in the legend of Fig. 7. The shown images are representative of three independent experiments. 100 × total magnification (10 × objective and a 10 × eyepiece). Inset: higher magnifications of merged images showing rhodamine-dependent cytoplasmic fluorescence emission by cell monolayers.
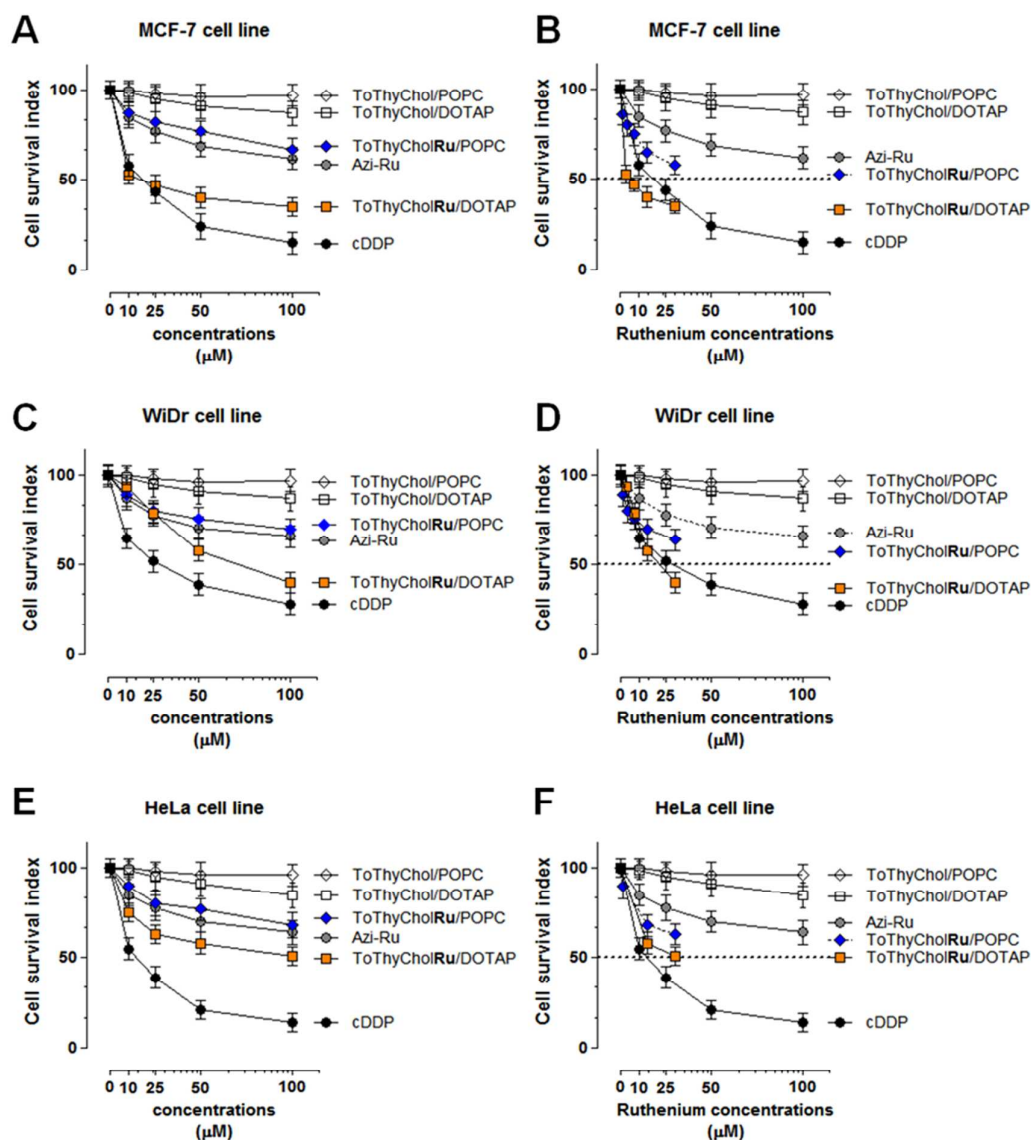
Fig. 9. Cell survival index, evaluated by the MTT assay and monitoring of live/dead cell ratio, for MCF-7 (panel A), WiDr (panel C), and HeLa (panel E) cell lines following 48 h of incubation with the indicated concentration (the range 10→1000 μM has been explored, the one 10→100 μM is shown) of AziRu and of the ruthenium-containing ToThyCholRu/DOTAP and ToThyCholRu/POPC liposomes, as indicated in the legend. Cisplatin (*cDDP*) is the positive control for cytotoxicity whilst the ruthenium-free ToThyChol/POPC and ToThyChol/DOTAP liposomes are added as negative controls. Panels B, D, and F show the corresponding concentration-effect curves by normalizing for the actual ruthenium amount contained within ToThyCholRu/DOTAP and ToThyCholRu/POPC liposomes. Data are expressed as percentage of untreated control cells and are reported as mean of five independent experiments ± SEM ($n = 30$).
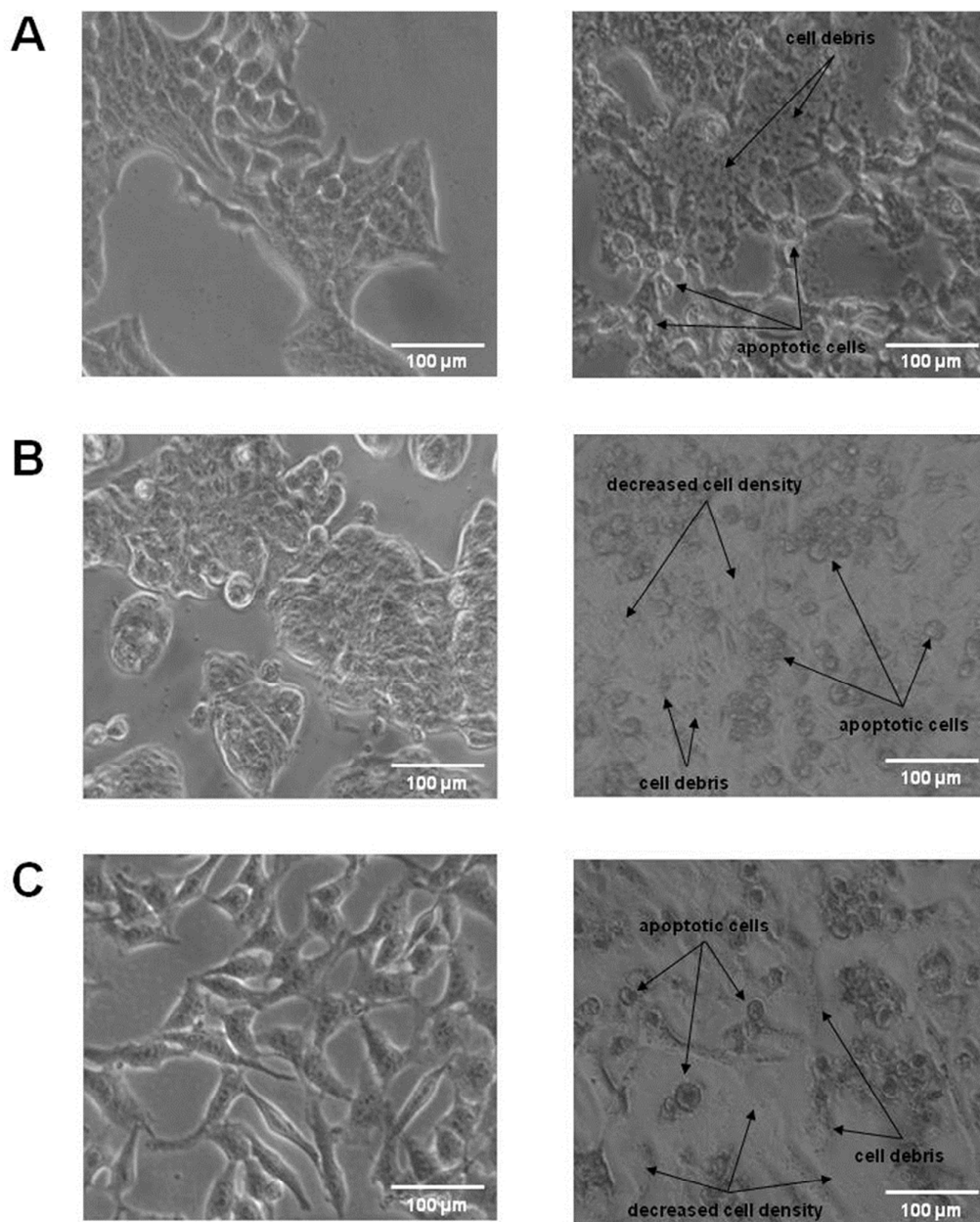
Fig.10. Representative microphotographs at a 200 × magnification (20 × objective and a 10 × eyepiece) by phase-contrast light microscopy of MCF-7 (panel A), WiDr (panel B) and HeLa (panel C) cell lines untreated (control cells, left column) or treated for 48 h with 50 µM ToThyCholRu/DOTAP (right column), showing the morphological changes of cells and the cytotoxic effects on cellular monolayers. The shown images are representative of three independent experiments.
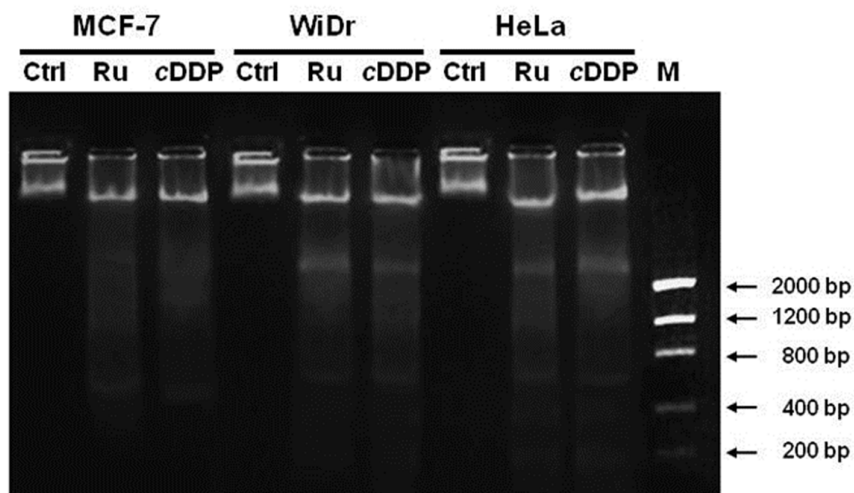
Fig. 11. DNA fragmentation assay on MCF-7, WiDr and HeLa cells, treated or not (Ctrl) for 48 h with IC$_{50}$ doses (13, 23, and 34 µM, respectively) of ToThyCholRu/DOTAP (Ru) or with IC$_{50}$ doses (22, 32, and 12 µM, respectively) of cisplatin (cDDP) as positive control for DNA fragmentation. After incubations, DNA was extracted and visualized on 1.5% agarose gel as detailed in the experimental section. Lane M corresponds to molecular weight markers. The agarose gel is representative of three independent experiments.

References

1. A. Bergamo, C. Gaiddon, J. H. M. Schellens, J. H. Beijnen and G. Sava, *J. Inorg. Biochem.*, 2012, 106, 90-99.
2. S. Komeda and A. Casini, *Curr. Top. Med. Chem.*, 2012, 12, 219-235.
3. A. Bergamo and G. Sava, *Dalton Trans.*, 2011, 40, 7817-7823.
4. L. Kelland, *Nat. Rev. Cancer*, 2007, 7, 573-584.
5. M. H. Ryu and Y. K. Kang, *Expert Rev. Anticanc.*, 2009, 9, 1745-1751.
6. E. Saloustros and V. Georgoulias, *Expert Rev. Anticanc.*, 2008, 8, 1207-1222.
7. G. Muhlgassner, C. Bartel, W. F. Schmid, M. A. Jakupec, V. B. Arion and B. K. Keppler, *J. Inorg. Biochem.*, 2012, 116, 180-187.
8. M. Groessl, Y. O. Tsybin, C. G. Hartinger, B. K. Keppler and P. J. Dyson, *J. Biol. Inorg. Chem.*, 2010, 15, 677-688.
9. S. M. Guichard, R. Else, E. Reid, B. Zeitlin, R. Aird, M. Muir, M. Dodds, H. Fiebig, P. J. Sadler and D. I. Jodrell, *Biochem. Pharmacol.*, 2006, 71, 408-415.
10. O. Mazuryk, K. Kurpiewska, K. Lewinski, G. Stochel and M. Brindell, *J. Inorg. Biochem.*, 2012, 116, 11-18.
11. E. Alessio, A. S. O. Santi, P. Faleschini, M. Calligaris and G. Mestroni, *Dalton Trans.*, 1994, 1849-1855.
12. G. Sava and A. Bergamo, *Anticancer Res*, 1999, 19, 1117-1124.
13. M. Bacac, A. C. G. Hotze, K. van der Schilden, J. G. Haasnoot, S. Pacor, E. Alessio, G. Sava and J. Reedijk, *J. Inorg. Biochem.*, 2004, 98, 402-412.
14. M. Vaccaro, R. Del Litto, G. Mangiapia, A. M. Carnerup, G. D'Errico, F. Ruffo and L. Paduano, *Chem. Commun.*, 2009, 1404-1406.
15. L. Simeone, G. Mangiapia, G. Vitiello, C. Irace, A. Colonna, O. Ortona, D. Montesarchio and L. Paduano, *Bioconjugate Chem.*, 2012, 23, 758-770.
16. G. Mangiapia, G. D'Errico, L. Simeone, C. Irace, A. Radulescu, A. Di Pascale, A. Colonna, D. Montesarchio and L. Paduano, *Biomaterials*, 2012, 33, 3770-3782.
17. G. Mangiapia, G. Vitiello, C. Irace, R. Santamaria, A. Colonna, R. Angelico, A. Radulescu, G. D'Errico, D. Montesarchio and L. Paduano, *Biomacromolecules*, 2013, 14, 2549-2560.
18. D. Montesarchio, G. Mangiapia, G. Vitiello, D. Musumeci, C. Irace, R. Santamaria, G. D'Errico and L. Paduano, *Dalton Trans.*, 2013, 42, 16697-16708.
19. A. Gissot, M. Camplo, M. W. Grinstaff and P. Barthelemy, *Org. Biomol. Chem.*, 2008, 6, 1324-1333.
20. G. Mangiapia, M. Vaccaro, G. D'Errico, H. Frielinghaus, A. Radulescu, V. Pipich, A. M. Carnerup and L. Paduano, *Soft Matter*, 2011, 7, 10577-10580.
21. A. Bajaj, S. K. Mishra, P. Kondaiah and S. Bhattacharya, *Biochim. Biophys. Acta, Biomembranes*, 2008, 1778, 1222-1236.
22. A. Bajaj, P. Kondaiah and S. Bhattacharya, *Bioconjugate Chem.*, 2007, 18, 1537-1546.
23. S. Bhattacharya and S. Haldar, *Biochim. Biophys. Acta, Biomembranes*, 2000, 1467, 39-53.
24. S. Bhattacharya and S. Haldar, *Biochim. Biophys. Acta, Biomembranes*, 1996, 1283, 21-30.
25. D. Musumeci and D. Montesarchio, *Molecules*, 2012, 17, 12378-12392.
26. M. K. Bijsterbosch, E. T. Rump, R. L. A. De Vrueh, R. Dorland, R. van Veghel, K. L. Tivel, E. A. L. Biessen, T. J. C. van Berkel and M. Manoharan, *Nucleic Acids Res.*, 2000, 28, 2717-2725.
27. A. M. Krieg, J. Tonkinson, S. Matson, Q. Y. Zhao, M. Saxon, L. M. Zhang, U. Bhanja, L. Yakubov and C. A. Stein, *Proc. Natl. Acad. Sci USA*, 1993, 90, 1048-1052.
28. M. Castaldi, L. Costantino, O. Ortona, L. Paduano and V. Vitagliano, *Langmuir*, 1998, 14, 5994-5998.
29. A. Lomakin, D. B. Teplow and G. B. Benedek, *Methods Mol. Biol.*, 2005, 299, 153-174.

30.   F. Fiorito, C. Irace, A. Di Pascale, A. Colonna, G. Iovane, U. Pagnini, R. Santamaria and L. De Martino, *Plos One*, 2013, 8.

31.   R. Angelico, L. Ambrosone, A. Ceglie, I. Losito, G. De Zio and F. Palmisano, *Phys. Chem. Chem. Phys.*, 2010, 12, 7977-7987.

32.   A. Merlino, G. Vitiello, M. Grimaldi, F. Sica, E. Busi, R. Basosi, A. M. D'Ursi, G. Fragneto, L. Paduano and G. D'Errico, *J. Phys. Chem. B*, 2012, 116, 401-412.

33.   G. Vitiello, G. Fragneto, A. A. Petruk, A. Falanga, S. Galdiero, A. M. D'Ursi, A. Merlino and G. D'Errico, *Soft Matter*, 2013, 9, 6442-6456.

34.   G. Fragneto, J. R. Lu, D. C. McDermott, R. K. Thomas, A. R. Rennie, P. D. Gallagher and S. K. Satija, *Langmuir*, 1996, 12, 477-486.

35.   G. D'Errico, A. Silipo, G. Mangiapia, G. Vitiello, A. Radulescu, A. Molinaro, R. Lanzetta and L. Paduano, *Phys. Chem. Chem. Phys.*, 2010, 12, 13574-13585.

36.   G. Vitiello, S. Di Marino, A. M. D'Ursi and G. D'Errico, *Langmuir*, 2013, 29, 14239-14245.

37.   D. Marsh, *Biochim. Biophys. Acta, Biomembranes*, 2010, 1798, 688-699.

38.   M. J. Swamy and D. Marsh, *Biochemistry-Us*, 1994, 33, 11656-11663.

39.   G. Vitiello, A. Falanga, M. Galdiero, D. Marsh, S. Galdiero and G. D'Errico, *Biochim. Biophys. Acta, Biomembranes*, 2011, 1808, 2517-2526.

40.   M. Groessl, O. Zava and P. J. Dyson, *Metallomics*, 2011, 3, 591-599.

41.   A. Bergamo and G. Sava, *Dalton Trans.*, 2007, 1267-1272.

42.   V. Brabec and O. Novakova, *Drug Resistance Updates*, 2006, 9, 111-122.

43.   J. Reedijk, *Eur. J. Inorg. Chem.*, 2009, 1303-1312.

44.   F. Mendes, M. Groessl, A. A. Nazarov, Y. O. Tsybin, G. Sava, I. Santos, P. J. Dyson and A. Casini, *J. Med. Chem.*, 2011, 54, 2196-2206.

45.   A. Casini, M. C. Diawara, R. Scopelliti, S. M. Zakeeruddin, M. Gratzel and P. J. Dyson, *Dalton Trans.*, 2010, 39, 2239-2245.

46.   L. Hosta-Rigau, Y. Zhang, B. M. Teo, A. Postma and B. Stadler, *Nanoscale*, 2013, 5, 89-109.

47.   B. Moghaddam, M. H. Ali, J. Wilkhu, D. J. Kirby, A. R. Mohammed, Q. G. Zheng and Y. Perrie, *Int. J. Pharm.*, 2011, 417, 235-244.

48.   F. Xiong, Z. Mi and N. Gu, *Pharmazie*, 2011, 66, 158-164.

49.   R. Simstein, M. Burow, A. Parker, C. Weldon C and B. Beckman, *Exp. Biol. Med. (Maywood)*, 2003, 228, 995-1003

50.   M. I. Webb, R. A. Chard, Y. M. Al-Jobory, M. R. Jones, E. W. Y. Wong and C. J. Walsby, *Inorg. Chem.*, 2012, 51, 954-966.

51.   C. P. Tan, S. S. Lai, S. H. Wu, S. Hu, L. J. Zhou, Y. Chen, M. X. Wang, Y. P. Zhu, W. Lian, W. L. Peng, L. N. Ji and A. L. Xu, *J. Med. Chem.*, 2010, 53, 7613-7624.

52.   D. V. Krysko, T. Vanden Berghe, K. D'Herde and P. Vandenabeele, *Methods*, 2008, 44, 205-221.

53.   J. A. Collins, C. A. Schandl, K. K. Young, J. Vesely and M. C. Willingham, *J. Histochem. Cytochem.*, 1997, 45, 923-934.

54.   R. U. Jänicke, M. L. Sprengart, M. R. Wati and A. G. Porter, *J. Biol. Chem.*, 1998, 273(16), 9357-9360.

55.   Y. Liang, C. Yan and N. F. Schor, *Oncogene,* 2001, 20(45): 6570-6578.

56.   M. Okamura, K. Hashimoto, J. Shimada and H. Sakagami, *Anticancer Res.*, 2004, 24, 655-661.

57.   C. P. Tan, S. H. Wu, S. S. Lai, M. X. Wang, Y. Chen, L. J. Zhou, Y. P. Zhu, W. Lian, W. L. Peng, L. N. Ji and A. L. Xu, *Dalton Trans.*, 2011, 40, 8611-8621.

58.   A. P. de Lima, F. D. Pereira, C. A. S. T. Vilanova-Costa, J. R. Soares, L. C. G. Pereira, H. K. P. Porto, L. A. Pavanin, W. B. dos Santos and E. D. Silveira-Lacerda, *Biological Trace Element Research*, 2012, 147, 8-15.

59.   L. Simeone, G. Mangiapia, C. Irace, A. Di Pascale, A. Colonna, O. Ortona, L. De Napoli, D. Montesarchio and L. Paduano, *Mol. Biosyst.*, 2011, 7, 3075-3086.
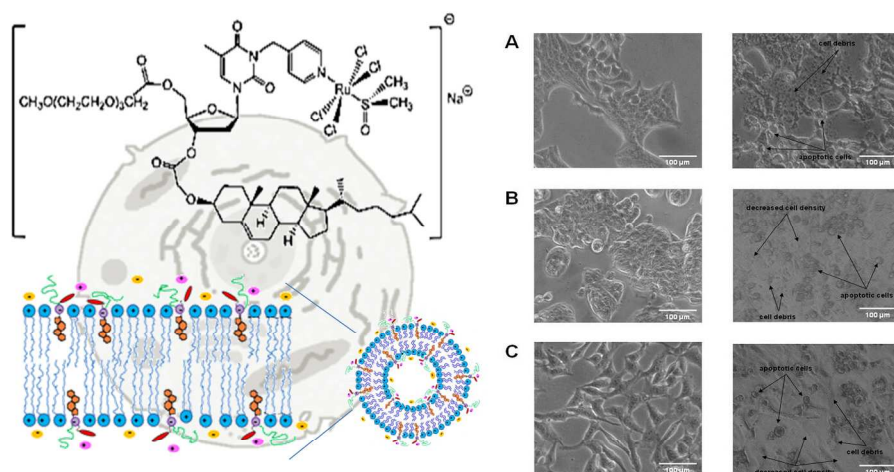
Cationic nanovectors loaded with ruthenium-based nucleolipids containing a cholesterol residue exert high growth-inhibitory activity against human cancer cells (MCF-7 (A), WiDr (B), and HeLa (C), before and after ToThyCholRu/DOTAP treatment).
1587x1190mm (96 x 96 DPI)